ESTIMATION OF SEISMIC DAMAGE FOR BRIDGES USING HAZARD MAPS

Takashi Sato[1] and Hiroaki Nishi[2]

Abstract

In addition to direct structural damage, secondary damage caused by structural dysfunction must also be considered. Damage to bridges, tunnels and other road elements may cause road closures that hinder rescue activities (such as victim evacuation and relief supply transportation) and restoration/recovery activities.

It is therefore necessary to estimate the wide-area structural damage conditions expected when earthquakes occur in an area and to take appropriate measures in advance to prevent secondary damage.

This study focused on a method of estimating earthquake damage to structures using hazard maps, and damage to bridge structures was estimated for the Hokkaido area – a region of Japan with a relatively high risk of earthquakes.

The earthquake hazard maps produced enabled earthquake load calculation depending on assumed earthquakes and two-dimensional identification of the corresponding damage to bridge structures. These maps can also be used effectively in evaluating anti-seismic reinforcement for bridges and repair priority, as well as in considering repair and reinforcement methods.

Introduction

Japan is one of the world's most earthquake-prone countries, and a variety of its structures have been damaged by large-scale tremors. Accordingly, it is important to minimize such damage through seismic design using seismic loads depending on regional characteristics and the importance of structures as well as by improving structural earthquake resistance through anti-seismic reinforcement and repair.

In addition to direct structural damage, secondary damage caused by structural dysfunction must also be considered. Damage to bridges, tunnels and other road elements may cause road closures that hinder rescue activities (such as victim evacuation and relief supply transportation) and restoration/recovery activities.

It is therefore necessary to estimate the wide-area structural damage conditions expected when earthquakes occur in an area and to take appropriate measures in advance to prevent secondary damage.

One way of ascertaining estimated damage over an entire target area is to use a hazard map. Under this method, the wide-area earthquake load is first estimated by considering the earthquake risk and ground characteristics of the target area. By combining multiple tremors and changing combinations, it is possible to define the

[1] Researcher, Civil Engineering Research Institute for Cold Region (CERI), PWRI
[2] Ph.D.eng., Team Leader, CERI, PWRI

earthquake risk depending on the purpose. Next, indexes of seismic structural damage are created based on the characteristics of structures and past seismic damage. Through such estimation using earthquake loads and seismic damage indexes and by plotting the results on a map, the conditions of damage resulting from an assumed earthquake can be identified two-dimensionally.

This paper presents the results of estimating seismic damage for bridge structures in Hokkaido (an area of Japan with a relatively high risk of earthquakes) using hazard maps and two-dimensional verification of damage conditions depending on assumed tremors.

Hazard map overview

Preparation methods for hazard maps and the details to be displayed on them vary by purpose and usage. Some display maximum acceleration, seismic intensity and other indicators of earthquake vibration magnitude, while others show the collapse of buildings, liquefaction and other damage conditions.

The hazard maps produced in this study are intended for use as basic materials in planning various post-earthquake measures by estimating seismic damage to structures based on the load of an assumed tremor and using structural damage indexes, and indicate both the earthquake load and structural damage conditions.

Figure 1 shows the algorithm for hazard map production. It consists of three parts – preparation of structural damage indexes, estimation of earthquake loads and estimation of seismic damage.

(1) Preparation of structural damage indexes

Since seismic performance varies by structure due to the variety of conditions involved (even for the same types of bridge, etc.), structures were first classified in accordance with the design criteria. Next, correlation analysis was conducted using past earthquake motion and damage data to identify the damage indexes of structures from earthquake loads with relatively good correlations, and the damage index levels were determined by considering the likelihood of damage as estimated from the classified seismic performance.

(2) Estimation of earthquake loads

To allow the setting of earthquake loads in the area for which the hazard map was to be produced, active faults, subduction zones and other seismic sources in the area were first identified to determine their positions and geometric forms, as well as the magnitude of earthquakes. Next, the target area of the hazard map was divided into meshes, and the earthquake load of the engineering bedrock in each section as applied from the above sources was calculated using an attenuation relation. The earthquake load at the ground surface was calculated by multiplying the load at the engineering bedrock by the predetermined earthquake amplification rate for each type of surface ground. If there were

multiple seismic sources, the maximum value of the load calculated for each source was adopted as the earthquake load in the mesh.

(3) Estimation of seismic damage

Structures in the target area of the hazard map were identified, and the seismic performance of each one was found based on the type of structure, the applicable design criteria and other factors. Structures were classified based on this seismic performance, and the seismic damage to them was estimated from the damage index depending on the seismic performance of each structure and the earthquake load at the relevant construction site. The results were plotted on the hazard map.
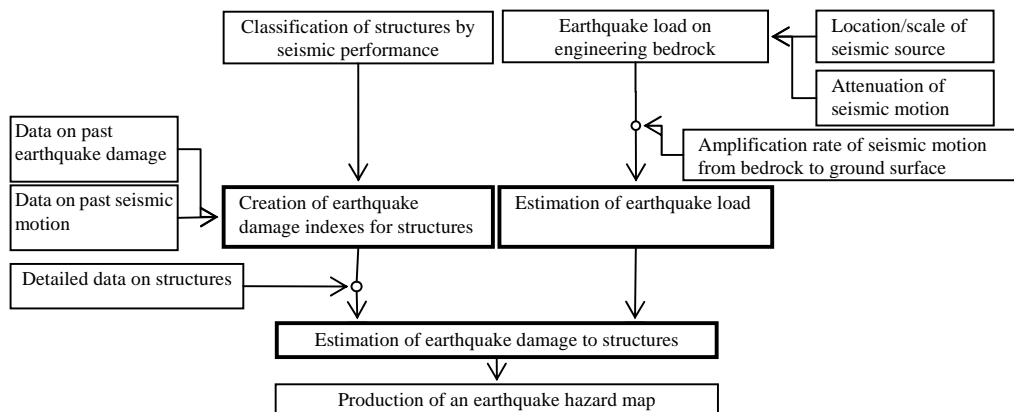
Figure 1 Algorithm for hazard map creation

Establishment of seismic damage indexes for bridge structures

The degree of seismic damage to bridge structures was determined by combining the structural characteristics of each structure with the relevant earthquake motion. Since such motion includes multiple factors (e.g., period/phase characteristics and duration), it is difficult to predict damage conditions accurately with a single load index. However, it is considered possible to forecast these conditions easily using earthquake motion indexes that are highly correlated to the damage.

(1) Classification of structures by seismic performance

Figure 2 shows the classification method for prediction of seismic damage to bridges. Seismic performance varies by the year of construction due to aging-related problems and differences in design criteria. **Table 1** shows the changes in seismic design criteria for bridge structures. The two revisions in 1971 and 1996, in which the setting of seismic force was changed considerably, are seen as the boundaries of seismic performance. Advancement of the design system can be seen in the revision of 1971, which provided more detailed seismic design loads and measures to prevent bridge

collapse. In the revision of 1996, the input earthquake motion for the design was increased by a factor of three to four based on damage resulting from the 1995 South Hyogo Prefecture Earthquake. Accordingly, these two years were set as the damage index boundaries. For bridges whose design criteria were unknown, two years before the time of construction was assumed to be the design year, and the closest design criteria before this time were assumed to have been used.

Anti-seismic reinforcement work has also been conducted for a variety of structures since the 1995 South Hyogo Prefecture Earthquake. The level of seismic performance was therefore set higher for bridges with anti-seismic reinforcement even if they were old.

Table 2 shows an example of summarizing the seismic performance set here for bridge structure data. It consists of the information, location (latitude, longitude), year of construction and seismic performance of the roads on which the bridge structures were built. The targets of this study were approximately 2,200 bridges over national highways in Hokkaido.
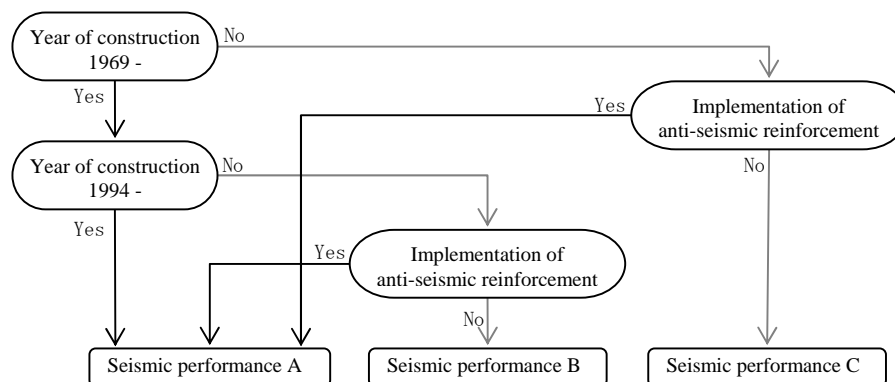
Figure 2 Flow chart of performance classification for bridge structure seismic performance

(2) Seismic damage indexes for bridge structures

Table 3 shows the proposed damage indexes for bridge structures. The necessity of repair to ensure trafficability serves as a guide to distinguishing the level of seismic damage to such structures. Accordingly, three indexes were used in this study for classification – Index I for non-damaged bridges, Index II for those with minor damage not requiring repair to ensure trafficability, and Index III for those with serious damage (e.g., shear failure of piers) requiring large-scale repair.

Structural damage is affected not only by the maximum values of acceleration, velocity and other earthquake motion factors but also by the period/phase characteristics and duration of earthquake motion. However, since it is difficult to model these characteristics simply, seismic damage was estimated in this study from the maximum velocity, which was found to be quite highly correlated with damage in past analysis. Based on previous studies conducted by the authors [Sato, T. et al., (2006)], three values

(35 cm/s on the safe side from the value at which minor damage is observed, 50 cm/s (the value provided as Level 2 earthquake motion by the Architectural Institute of Japan), and 100 cm/s (the value observed at the time of the 1995 South Hyogo Prefecture Earthquake)) were used as the standards for damage index classification.

Earthquake load classification and classification by the seismic performance of structures based on seismic design criteria were comprehensively evaluated to produce the damage indexes shown in **Table 3**.

Table 1 Changes in the bridge structure seismic design code

Series	Year of revision	External force	Verification method
1926 (T15)	1926	Strongest seismic motion at the location	Allowable stress design method
1939 (S14)	1939	20% horizontal and 10% vertical load of the dead weight Conditions of the construction site must be considered.	Allowable stress design method
1956 (S31)	1956	Horizontal seismic intensity must be considered depending on ground conditions and regions. (Introduction of the coefficient of regional difference)	Allowable stress design method
1971 (S46)	1971	Change in the calculation method for horizontal seismic intensity	Allowable stress design method
1981 (S56)	1981	Change in the coefficient of regional difference	Allowable stress design method
1990 (H2)	1990	Change of ground types	Introduction of the ultimate earthquake resistance method
1996 (H8)	1996	Change in external force	Verification of design and horizontal load bearing capacity during earthquakes using the seismic coefficient method

T: Taisho; S: Showa; H: Heisei (names of Japanese eras)

Table 2 Sample bridge data

Bridge	National route	Longitude	Latitude	Year of construction	Seismic performance
Bridge A	36	141.4	43.1	1966	C
Bridge B	36	141.3	43.0	1972	C
Bridge C	230	141.3	43.0	1994	B
Bridge D	230	141.2	43.0	1961	C
Bridge E	231	141.4	43.2	1972	C
Bridge F	231	141.4	43.2	1991	B
Bridge G	231	141.3	43.2	1990	B
Bridge H	12	141.8	43.2	1973	C
Bridge I	12	141.9	43.3	1967	C

Table 3 Bridge structure seismic damage index

Seismic Performance	Max. velocity(cm/s)			
	35	50	100	
A	I	I	I	II
B	I	II	II	III
C	I	II	III	III

I: Undamaged bridges
II: Bridges with minor damage not requiring repair
III: Bridges with serious damage requiring large-scale repair (e.g., shear failure of bridge piers)

Estimation of earthquake loads

　　To determine the earthquake loads to be used for hazard maps, it is necessary to estimate the maximum earthquake motion in each area. This value varies by the setting of the location and shape of the seismic source, the magnitude of the earthquake and other initial conditions. Even if the seismic source is the same, earthquake motion observed at the ground surface varies greatly depending on landform, ground conditions and other regional characteristics. This section identifies the seismic sources affecting Hokkaido, and outlines earthquake motion estimation taking account of site characteristics by using surface ground types.

(1) Seismic sources in and around Hokkaido

　　Figure 3 shows the epicenter distribution of earthquakes with a seismic intensity of 3 or higher on the Japanese scale that have occurred around Hokkaido (1924 – 2009). The darker parts indicate areas where many earthquakes have occurred. It can be seen that, while seismic sources are observed throughout Hokkaido, they are basically concentrated in certain areas, such as along the subduction zone on the Pacific coast and the eastern margin of the Sea of Japan. In the subduction zone, many earthquakes have occurred in the eastern offing of the Nemuro Peninsula.

　　Although records of inland-type earthquakes in Hokkaido are scarce, the sources of such tremors were included among the targets because extremely large earthquake motion is generated around these sources when they do occur.

　　Based on the above, the seismic sources affecting earthquake risk in Hokkaido were classified into four types – HA (inland active fault), HB (subduction zone of the Pacific coast plate), HC (eastern margin of the Sea of Japan) and HD (other). **Figure 4** and **Table 3** show the target seismic sources along with magnitude values and other details of earthquakes.
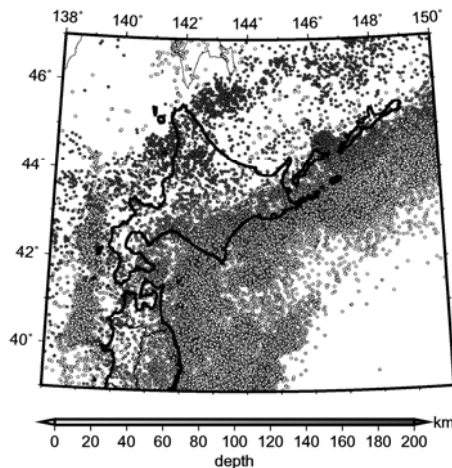
Figure 3 Epicenter distribution map of earthquakes around Hokkaido, Japan (Mj => 3.0)
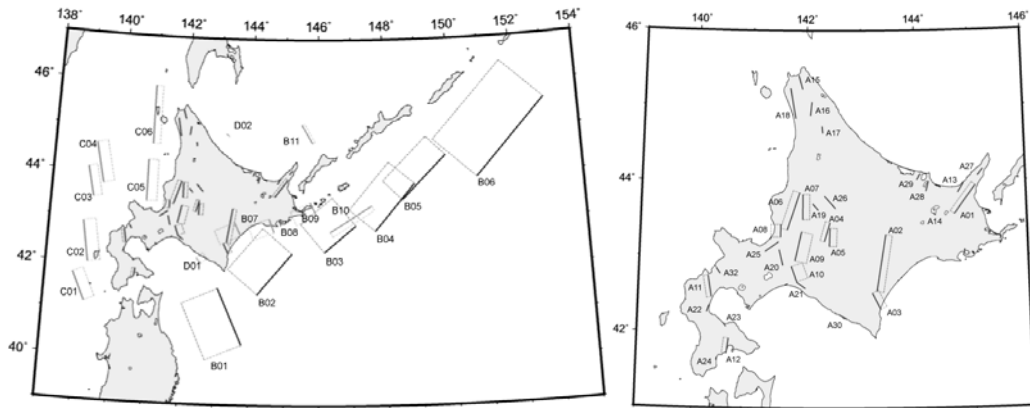
Figure 4 Seismic sources in Hokkaido and its surroundings
Table 3-1 Source model parameters

Type	No.	Magnitude		Length	Width	Fault coordinates		Depth	Strike	Dip
		Mj	Mw	km	km	Latitude	Longitude	km	deg.	deg.
Inland crustal earthquakes	A01	7.7	7.1	52.6	14.0	43.9425	145.0807	2.0	217.0	60
	A02	8.0	7.3	84.4	20.0	42.5470	143.2710	2.0	9.3	60
	A03	7.2	6.7	27.1	20.0	42.3070	143.3358	2.0	333.0	60
	A04	7.2	6.8	28.9	14.0	43.4540	142.4290	2.0	196.0	60
	A05	7.2	6.8	26.5	16.0	43.1465	142.4211	2.0	1.8	50
	A06	7.8	7.2	58.2	20.0	43.8546	141.8789	2.0	198.0	60
	A07	7.5	6.9	37.0	20.0	43.5000	141.9380	2.0	0.0	60
	A08	7.0	6.5	18.5	19.0	43.4330	141.5390	2.0	180.0	40
	A09a	-	7.3	43.6	24.0	42.9530	141.8000	2.0	12.6	45
	A09b	-	7.3	26.8	24.0	42.7490	141.8830	2.0	345.0	45
	A10	7.1	6.6	23.7	24.0	42.6760	141.8340	2.0	340.0	45
	A11	7.3	6.8	31.9	14.0	42.7469	140.2463	2.0	170.0	60
	A12	7.3	6.8	22.4	14.0	41.9191	140.6293	2.0	187.0	60
	A13	6.8	6.4	16.0	8.0	43.9689	144.8640	2.0	212.0	90
	A14	6.0	5.8	5.0	3.0	43.5774	144.3000	2.0	128.0	90
	A15	7.1	6.6	21.7	15.0	45.4090	141.8450	2.0	164.0	90
	A16	7.6	7.0	45.0	23.0	45.2371	141.6950	2.0	170.0	90
	A17	7.0	6.5	20.0	10.0	45.0541	142.0930	2.0	186.0	90
	A18	6.5	6.2	10.0	5.0	44.7327	142.2830	2.0	175.0	90
	A19	6.6	6.3	12.0	6.0	43.7065	142.1150	2.0	138.0	90
	A20	7.1	6.6	24.0	12.0	43.1000	141.5120	2.0	166.0	90
	A21	6.8	6.4	16.0	8.0	42.6702	141.8290	2.0	125.0	90
	A22	6.5	6.2	10.5	10.0	42.3540	140.2740	2.0	198.0	90
	A23	6.1	5.9	6.0	3.0	42.1197	140.5390	2.0	147.0	90
	A24	5.8	5.6	4.0	3.0	41.6652	140.4250	2.0	184.0	90
	A25	6.6	6.2	11.8	12.0	44.1510	145.2210	2.0	220.0	90
	A26	6.8	6.4	15.4	15.0	44.0010	144.2270	2.0	194.0	90
	A27	6.5	6.2	10.4	10.0	44.1020	144.0790	2.0	209.0	90
	A28	6.6	6.2	12.4	12.0	42.2410	142.5970	2.0	120.0	90
	A29a	7.2	6.7	10.8	15.0	42.8530	140.3880	2.0	147.0	90
	A29b	7.2	6.7	13.7	15.0	42.7710	140.4600	2.0	198.0	90
	A30	7.1	6.6	24	12	43.1998	141.5020	2.0	235	90
	A31	7.1	6.6	24	12	43.8075	142.3290	2.0	138	90

Table 3-2 Source model parameters

Type	No.	Magnitude		Length	Width	Fault coordinates		Depth	Strike	Dip
		Mj	Mw	km	km	Latitude	Longitude	km	deg.	deg.
Subduction zone earthquakes	B01	7.9	7.2	150	100	41.5500	143.0500	0	156	20
	B02	8.2	7.5	130	100	42.3300	145.2200	1	220	20
	B03	7.4	6.9	100	100	42.9400	147.1100	1	230	27
	B04	7.9	7.2	150	85	43.8500	148.8900	23	220	16
	B05	8.1	7.4	150	70	44.4500	149.8500	56	225	20
	B06	8.1	7.4	250	150	45.5900	152.9700	4	223	22
	B07	7.5	6.9	36	54	43.0000	143.5000	80	155	11
	B08	7.5	6.9	36	54	43.0907	144.5223	100	159	11
	B09	7.5	6.9	36	54	43.4500	145.7500	120	155	11
	B10	8.2	7.5	120	60	42.8000	146.3500	25	58	78
	B11	7.2	6.7	52	56	44.7400	145.8200	90	330	83
Earthquakes on the Sea of Japan's eastern margin	C01	7.0	6.5	75	30	41.1500	139.2000	10	335	25
	C02	7.5	6.9	100	35	42.0000	139.2300	10	350	30
	C03	7.0	6.5	75	30	43.4200	139.2600	10	347	45
	C04	7.5	6.9	100	35	43.7300	139.5300	10	347	40
	C05	7.0	6.5	100	35	43.4000	140.8500	10	0	45
	C06	7.5	6.9	140	24	44.6500	140.9500	20	0	45
Other types	D01	7.1	6.6	18	23	42.0800	142.5400	20	320	30
	D02	6.9	6.3	10	20	44.9300	143.1800	238	130	90
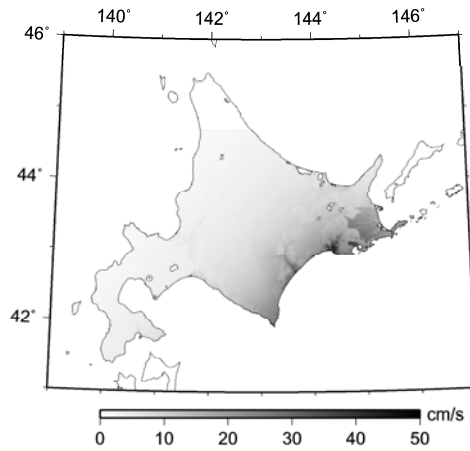
Figure 5 Example map showing preset earthquake loads
(Maximum velocity distribution at the surface layer assuming an earthquake
in the subduction zone on the Pacific coast)

(2) Caculation of maximum velocity in consideration of site characteristics

The earthquake load of each area with bridges depends mainly on the source of the tremor and its scale, as well as on the ground structure of the surface layer. It is therefore necessary to set an earthquake load for each bridge structure location.

In this study, the seismic source parameters were set based on past earthquakes in Hokkaido and other data [Sato, R.][2]. **Table 3** shows the parameters of each seismic

source. Using these parameters and the attenuation relationship outlined by Si and Midorikawa [Hongjun Si and Saburo Midorikawa], the maximum velocity of the engineering bedrock was calculated for sections divided into meshes. The resulting values were then multiplied by the amplification rate of the surface ground in Hokkaido as found by the authors in the past [Sato, T. et al., (2008)] to ascertain the maximum velocity of the surface layer.

In this study, earthquake motion distribution at the maximum velocity was calculated for the 42 seismic sources shown in **Table 1**. These results are used separately or in combination to produce earthquake load maps depending on their purpose. **Figure 5** shows a maximum velocity distribution map for the subduction zone on the Pacific side as an example of an earthquake load map.

Characteristics of hazard maps and variations in damage to bridges with differences in seismic source

Table 4 shows the numbers of bridge structures categorized for damage indexes by differences in seismic source. This section outlines the production of a hazard map for individual sources to verify the degree and distribution of expected damage. Since hazard map output for bridges requires data on such structures in the target area, bridge data including seismic performance figures (as shown in **Table 5** above) were created.

Table 4 Numbers of bridge structures categorized for damage indexes depending on differences in assumed earthquakes

Assumed earthquake	Damage index I	Damage index II	Damage index III
Inland crustal earthquake	1,666	336	215
Subduction zone earthquake	2,207	10	6
Earthquake on the Sea of Japan's eastern margin	2,215	2	9
Other types	2,217	0	0

(1) Damage to bridge structures assuming an inland crustal earthquake

Figures 6 (a) to **(c)** show maps for earthquake damage indexes I to III, respectively, assuming an inland crustal earthquake.

As can be seen from **Table 4**, the total of damage indexes I and III reached nearly 25% in the case of the assumed inland crustal earthquake HA. However, while such earthquakes are highly destructive, their rate of occurrence is extremely low. Accordingly, the results of estimation for this type of damage do not necessarily mean that all structures lack safety.

Looking at the areas where the assumed damage is concentrated in **Figs. 6 (b)** and (c), it can be seen that damaged bridges are concentrated around points where the maximum velocity exceeds 50 cm/s (i.e., faults). However, in **Fig. 6 (a)**, some bridges are categorized as damage index I (undamaged) around faults. It is therefore important to determine the priority of measures against damage in line with the results of estimation for damage to bridge structures, rather than assuming that all bridges located around faults will

sustain serious damage.

(a) Damage index I

(b) Damage index II
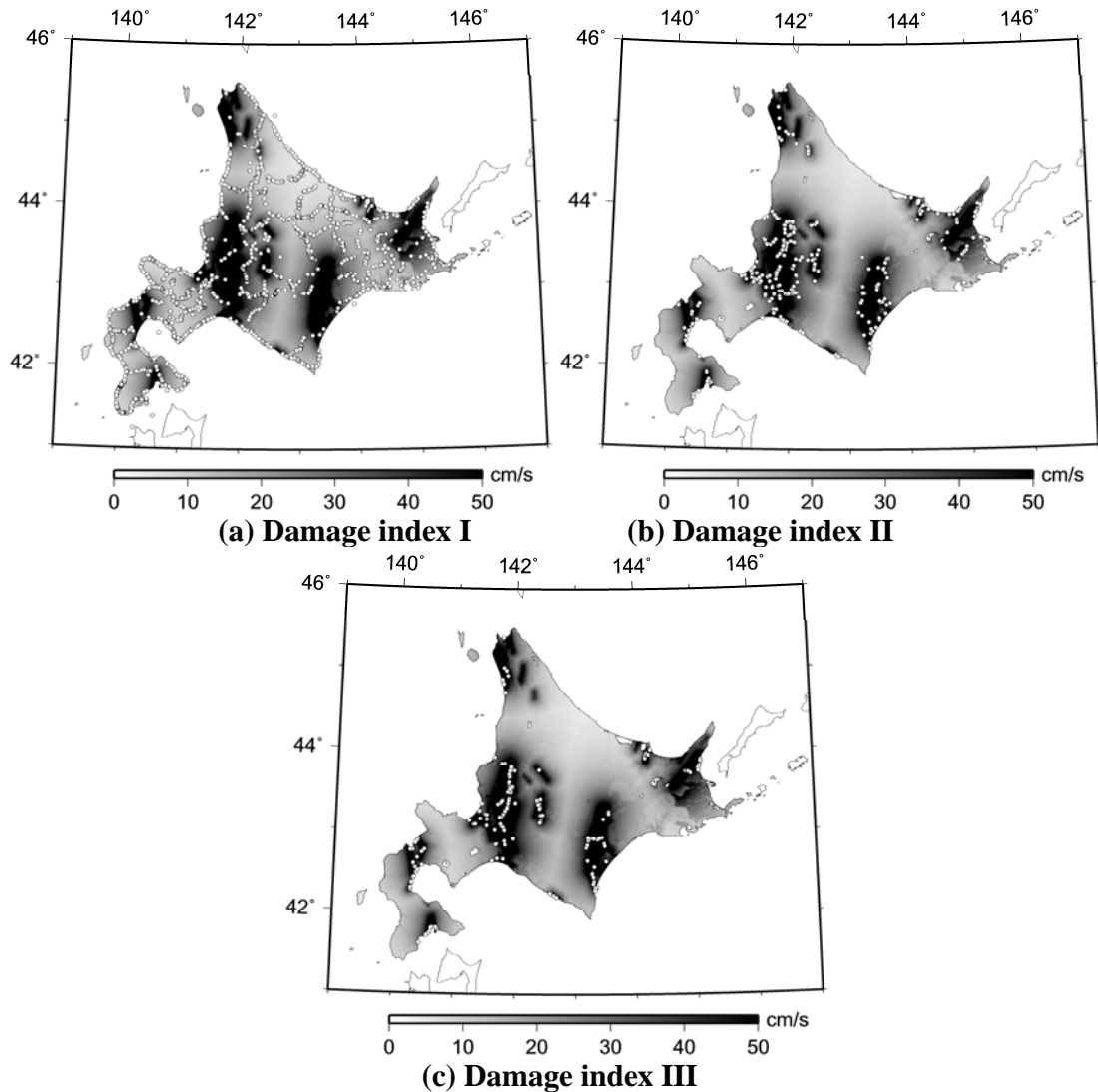
(c) Damage index III
Figure 6 Inland crustal earthquake hazard map for bridge structures

(2) Damage to bridges assuming a seismic source in the subduction zone on the Pacific coast

 Figures 7 (a) to **(c)** show maps for earthquake damage indexes I to III, respectively, assuming a seismic source in the subduction zone on the Pacific coast. For the assumed earthquake HB in this case, 10 bridges are categorized as damage index II and 6 as damage index III. Since the seismic source is on the Pacific coast, the earthquake load in the coastal zone becomes larger, causing damage to bridges in the area.
 Earthquakes in the subduction zone on the Pacific coast occur most frequently

around Hokkaido according to seismic records, and damage to bridges there was reported at the time of the 2003 Tokachi-oki Earthquake [Monthly Report of the CERI]. While the Chiyoda Ohashi bridge suffered relatively serious damage as a result of this tremor, damage to it in this study was minor (index I) in contrast to the actual damage conditions. The main reasons for this may be that the earthquake assumed in the study did not completely reproduce past tremors, and that the seismic performance of bridges is set only in a simplified manner. However, while simulated damage to individual bridge structures may differ from actual damage as mentioned above, past damage is roughly reproduced on the hazard map concerning the distribution of damaged bridges along the Pacific coast and the number of damaged bridges, indicating the effectiveness of the map in two-dimensional damage estimation.

(a) Damage index I   (b) Damage index II
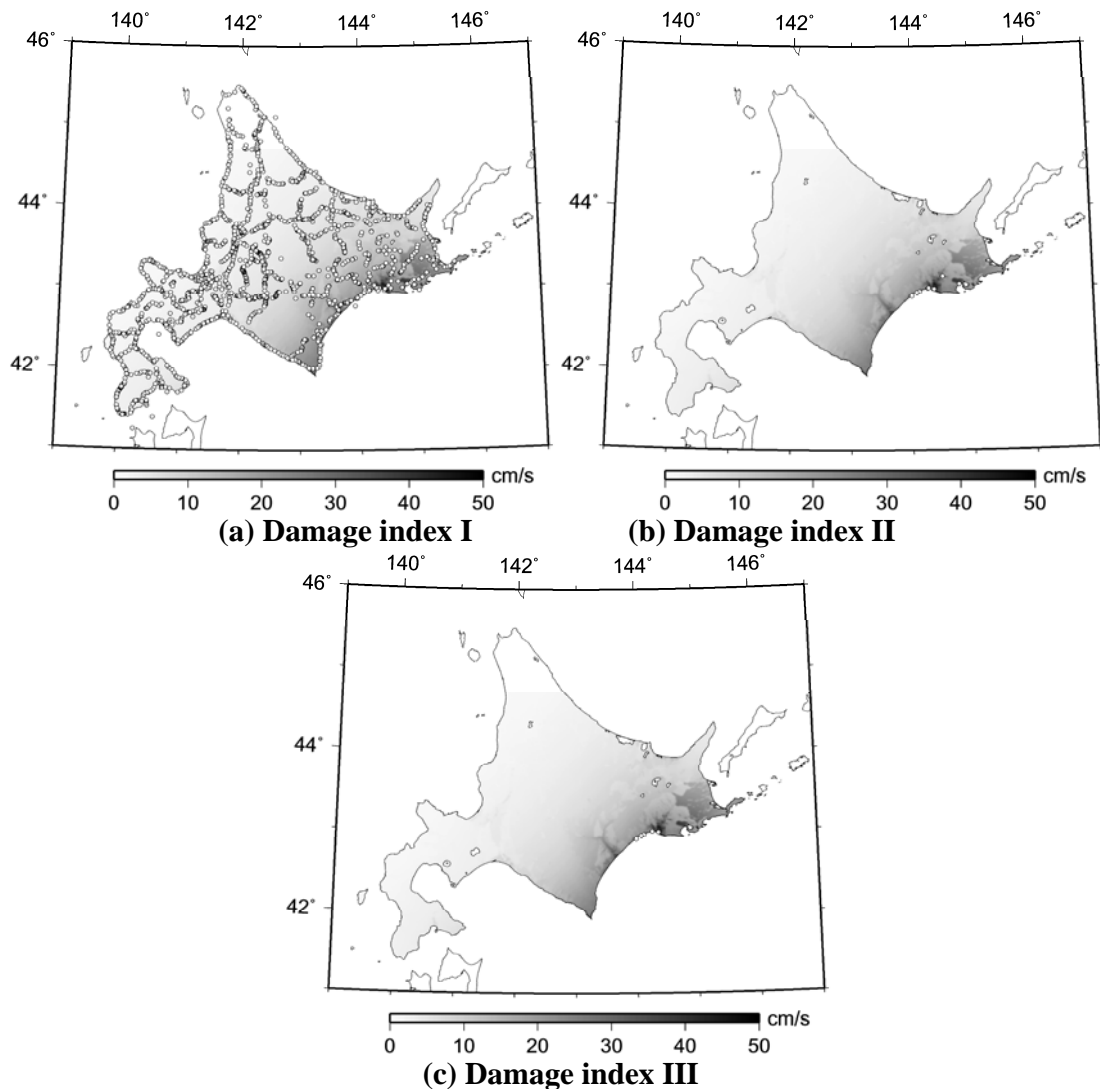
(c) Damage index III

Figure 7 Subduction zone earthquake hazard map for bridge structures

(3) Damage to bridges assuming a seismic source at the eastern margin of the Sea of Japan

   Figures 8 (a) to **(c)** show damage maps for earthquake damage indexes I to III, respectively, assuming a seismic source at the eastern margin of the Sea of Japan. A characteristic of the earthquake from this source is that more bridges are categorized as damage index III than II, indicating that bridges with low seismic performance are concentrated in the area where strong vibrations emanate from this seismic source.

(a) Damage index I
       (b) Damage index II

(c) Damage index III
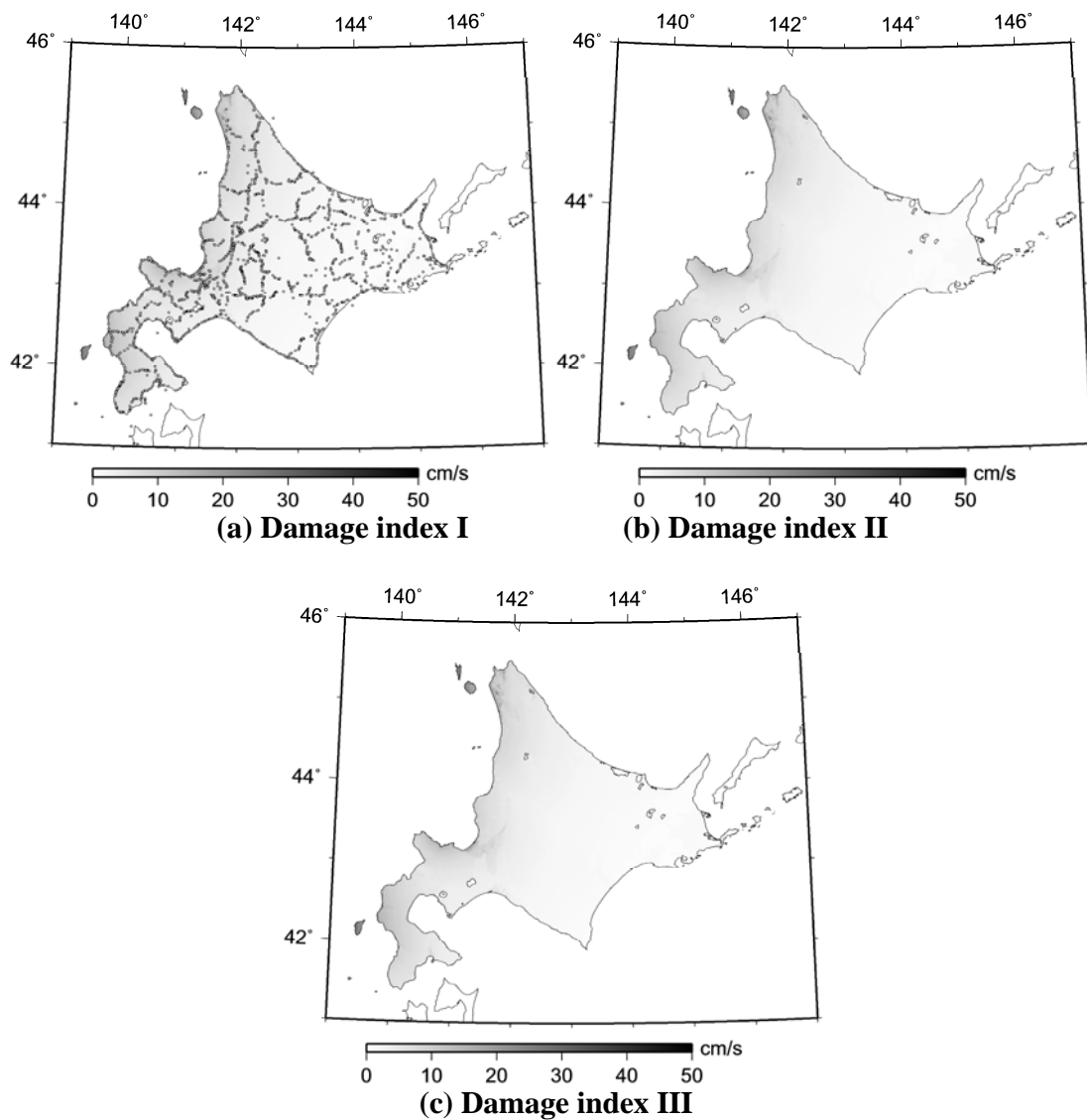
Figure 8 Sea of Japan eastern margin earthquake hazard map for bridge structures

(4) Damage to bridges assuming other seismic sources

As can be seen from **Table 4**, earthquakes with other seismic sources are deemed not to cause damage to bridge structures in the results based on these damage indexes. The damage maps for such earthquakes are therefore omitted.

Conclusion

To prevent secondary damage to bridges in earthquakes, it is necessary to monitor the damage conditions of structures two-dimensionally in advance and take appropriate measures. This study focused on a method of estimating earthquake damage to structures using hazard maps, and damage to bridge structures was estimated for the Hokkaido area – a region of Japan with a relatively high risk of earthquakes.

The earthquake hazard maps produced enabled earthquake load calculation depending on assumed earthquakes and two-dimensional identification of the corresponding damage to bridge structures. These maps can also be used effectively in evaluating anti-seismic reinforcement for bridges and repair priority, as well as in considering repair and reinforcement methods. In the future, it will be necessary to improve the accuracy of damage indexes and prepare multiple indexes to improve the accuracy of structural damage estimation.

References

Civil Engineering Research Institute of Hokkaido (CERI) , (2003), " Investigation Report on the 2003 Tokachi-oki Earthquake ", Monthly report of special issue.

Hongjun Si and Saburo Midorikawa (1999). " New Attenuation Relationships for Peak Ground Acceleration and Velocity Considering Effects of Fault Type and Site Condition ", AIJ Journal of Structural and Construction Engineering, No. 523, pp. 63 – 70, Sept.

Sato, R., (1989). " Handbook on Earthquake Faults in Japan ", Kashima Shuppankai.

Sato, T., Ikeda, T., Kamiakito, N. and Ishikawa, H., (2006). " Study on a Damage Index to Estimate the Damage of structure ", Proceedings of the Hokkaido Chapter of The Japan Society of Civil Engineers, No. 63, A-40.

Sato, T., Nishi, H., Kamiakito, N. and Ikeda, T., (2008). " Estimation of Surface Ground Amplification Using Seismic Observation Records in Hokkaido ", 54th Symposium of Structural Engineering, Vol. 54A, pp. 256-265.